Mon. Not. R. astr. Soc. (1992) **255**, *Short Communication*, 31P–36P

Silicate dust in a Vega-excess system

C. J. Skinner,[1,★] M. J. Barlow[2] and K. Justtanont[3]†

[1] *University of Manchester, Nuffield Radio Astronomy Laboratories, Jodrell Bank, Macclesfield, Cheshire SK11 9DL*
[2] *Department of Physics and Astronomy, University College London, Gower Street, London WC1E 6BT*
[3] *NASA–Ames Research Center, MS 245–3, Moffett Field, CA 94035, USA*

Accepted 1992 February 7. Received 1992 January 15; in original form 1991 October 31

SUMMARY

The 10-μm spectrum of the K5V star SAO 179815 (=HD 98800) is presented, and conclusively demonstrates the presence of small silicate dust grains (probably in a disc) around this star. The 9.7-μm silicate dust feature is unusually broad and shallow in this system. This, together with the slow fall-off of flux at longer wavelengths, constrains the size and density distributions of dust grains in models of the disc. We find that there must be a significant population of small grains (radii at least as small as 0.01 μm), as well as a population of large grains (radii at least as large as 100 μm) in order to explain all the observed properties of the disc.

Key words: circumstellar matter – stars: individual: SAO 179815 – dust, extinction – infrared: stars.

1 INTRODUCTION

The first evidence for protoplanetary discs in stellar systems similar to our own was the far-infrared excess in the spectrum of Vega, discovered during the *IRAS* mission (Aumann *et al.* 1984). Gillett (1986) subsequently described circumstellar excesses, determined from *IRAS* pointed observations, around three other main-sequence stars. Aumann (1985) identified, from *IRAS* survey observations, eight additional nearby 'Vega-excess' stars. Since then, the most extensively studied of such discs has been that around β Pictoris, owing to its size and proximity to the Solar System.

Smith & Terrile (1984) presented near-IR images of β Pic, whilst Paresce & Burrows (1987) obtained *BVRI* coronagraphic images of the disc. Artymowicz, Burrows & Paresce (1989) constructed detailed models to account for the optical properties of the disc by scattering off the dust grains, with the far-IR fluxes produced by thermal emission from the same grains. Unfortunately, the assumed properties of the grains do not resemble measured laboratory properties of dust grains. Their results may thus be treated with some caution; there is in any case some question as to the uniqueness of their model results.

On the basis of their models, Artymowicz *et al.* suggested that the grains are of a single size, and are either 'large' ($r_g > 20$ μm) or 'mid-size' ($1 < r_g < 20$ μm). Their results indicate that the grain radii are principally in the range $1 < r_g < 20$ μm, and that the dust grain number density varies as the inverse cube of distance from the central star (i.e. $\rho_g \propto r^{-3}$). On the basis of submillimetre observations, Becklin & Zuckerman (1990) suggested that the radii of the principal radiating grains lie in the range $3 < r_g < 100$ μm for Vega and α PsA, and $r_g < 3$ μm for β Pic.

Using a bolometer array, Telesco *et al.* (1988) resolved the β Pic disc at 10.8 and 19.2 μm, confirming that the dust radiating at these wavelengths is indeed physically associated with that scattering optical radiation in the disc. With the same instrument, Telesco & Knacke (1991) for the first time obtained spectroscopic information at four wavelengths from narrow-band photometry ($\Delta\lambda = 1$ μm) between 8.5 and 12.5 μm. They inferred the presence of small silicate grains from the apparent presence of a 9.7-μm emission feature. Uncertainties in the slope of the underlying continuum led to some uncertainty in the shape of the short-wavelength side of the emission.

At this point, we are presented with the possible presence in these systems of an unspecified distribution of large, mid-size and small grains, which probably contain silicates as a constituent.

2 OBSERVATIONS

Walker & Wolstencroft (1988) published the most comprehensive list to date of suspected Vega-excess stars from the *IRAS* Point Source Catalogue (PSC). We observed one of these, SAO 179815 (HD 98800), on 1991 May 25.3 (UT) at

★ Present address: Institute for Geophysics and Planetary Physics, Lawrence Livermore National Laboratory, 7000 East Avenue, L-413, Livermore CA 94550, USA, and Laboratory for Experimental Astrophysics, Lawrence Livermore National Laboratory, 7000 East Avenue, L-401, Livermore, CA 94550, USA.
† Present address: Department of Physics and Astronomy, University College London, Gower Street, London WC1E 6BT.

the United Kingdom Infrared Telescope (UKIRT) using CGS3, a common-user 10- and 20-μm grating spectrometer built at University College London. CGS3 contains an array of 32 discrete As:Si photoconductive detectors, and three interchangeable, permanently mounted gratings covering the 7.5–13.5 and 16.0–24.5 μm wavebands. Two grating settings give a fully sampled 64-point spectrum of the chosen waveband. We took one spectrum, covering the 7.8–13.2 μm waveband at a spectral resolution of 0.17 μm, using a 5.5-arcsec beam. The telescope secondary was chopped east–west at 7 Hz with a 30-arcsec throw. A spectrum of α Boo was used for spectrophotometric calibration, whilst rotating sector chopper sky spectra were used for flat-fielding both spectra.

The resulting spectrum is presented in Fig. 1. Since the *IRAS* 12-μm PSC flux density is only 2.0 Jy, and the integration time per point was only 250 s, the error bars are somewhat large. We have not achieved complete cancellation of the atmospheric ozone band at around 9.6 μm. Nonetheless, silicate dust emission, peaking at around 10.0 μm, is clearly seen in our spectrum, and so we have conclusive evidence for the presence of small circumstellar silicate dust grains.

The *IRAS* 12-μm PSC flux point lies a little above our CGS3 spectrum; the uncertainty in the *IRAS* flux is about 10 per cent, and the uncertainty in the absolute photometric calibration of our spectrum is similar, so within the errors our spectrum and the *IRAS* datum are roughly consistent. We have not rescaled our spectrum to the *IRAS* flux, since it is unclear which lies closest to the 'true' flux. There is also the question of the colour correction to the *IRAS* flux, which will be determined later from our models.

3 ANALYSIS

Walker & Wolstencroft (1988) suggested that SAO 179815 has a circumstellar disc. Such a disc has been observed around the main-sequence star β Pic, and discs are widely assumed to surround Vega and a variety of other main-sequence stars. We are unable at present to prove that the dust surrounding SAO 179815 is in a disc as opposed to a spherical envelope or shell. However, in the case of main-sequence stars such as those listed by Walker & Wolstencroft, it is easier to explain the presence of a circumstellar disc in terms of the remains of the star formation process than dust in any other geometry, and we assume hereafter that this is the case.

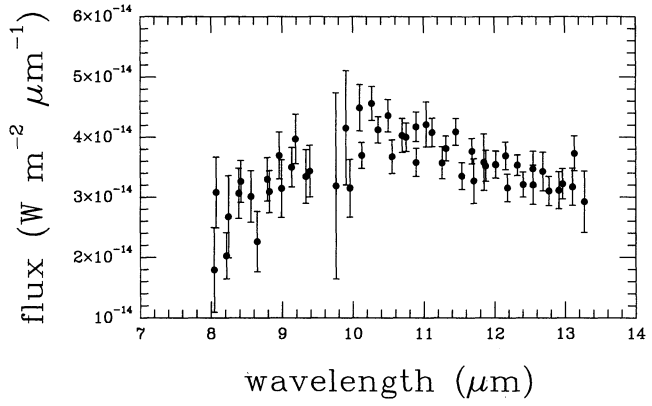

Figure 1. CGS3 spectrum of SAO 179815. The gap around 9.5 μm is due to incomplete cancellation of the atmospheric ozone feature.

In order to quantify the properties of the disc, we have constructed models to fit the observations. Our model for a protoplanetary disc follows that developed for the M supergiant α Orionis by Skinner & Whitmore (1987) in all respects other then geometry. In the present case we work in cylindrical geometry, making no allowance for possible variation in the disc thickness. Since the inner radii of these discs are generally large compared with the stellar diameters (Walker & Wolstencroft 1988), the effects of variable disc thickness on grain temperature distributions will be negligible, unless the disc is extremely thick, which we consider unlikely.

A power-law particle size distribution, caused by collisional fragmentation effects, has been predicted by Dohnanyi (1969, 1970) for asteroidal fragments and for micrometeoroids. We assume here a population of grains of different sizes, represented by $n_g \propto r_g^{-\alpha}$, where n_g is the number of grains of radius r_g. In the interstellar medium the value of α is normally taken to be 3.5, as determined by Mathis, Rumpl & Nordsieck (1977). The same size distribution is predicted theoretically by Biermann & Harwit (1980), from the effects of grinding together of grains in environments such as molecular clouds or red giant winds. However, in a protoplanetary disc the likely grain size distribution is unknown. Initially one might expect the interstellar value to prevail, but with time small grains might be driven out of the disc by stellar radiation pressure, or spiral into the star due to Poynting–Robertson drag, very large grains (up to planet size!) may form and small grains may be re-formed by grain–grain collisions. We shall treat α as a free parameter to be determined.

The total dust density distribution in the disc as a function of distance from the star is allowed to vary as $\rho_d \propto r^{-\beta}$. Becklin & Zuckerman (1990) and Artymowicz *et al.* (1989) both favour a value of β close to 3; however, we allow β to remain a free parameter, since there is no obvious reason to expect any particular value.

The model spectra were convolved with the system response curves for the *IRAS* 12-, 25-, 60- and 100-μm survey instruments to determine the actual *IRAS* PSC fluxes appropriate to the models. Colour corrections were also calculated in each case.

A number of sources of optical constants for amorphous silicate dust grains are available (Skinner & Whitmore 1987). A few initial runs of our model indicated that the constants due to Draine & Lee (1984) were likely to produce the best fit, and we use only these henceforth. Other constants did not reproduce the observed shape of the silicate feature or peak wavelength so well. We arbitrarily modified the optical constants longwards of 25 μm so that the absorption efficiencies of small grains would fall as λ^{-1} rather than λ^{-2}, since this agrees better with many recent observational determinations. Models run with absorption efficiencies falling as λ^{-2} indicated that it would in no way be possible to generate enough flux at 60 and 100 μm to fit the observations. Mie theory was used to calculate extinction, scattering and absorption efficiencies for grains with radii from 0.005 to 10 000 μm. Scattering and extinction efficiencies as functions of wavelength and grain size are plotted in Fig. 2. As expected, as the grain size increases, the 9.7- and 18-μm

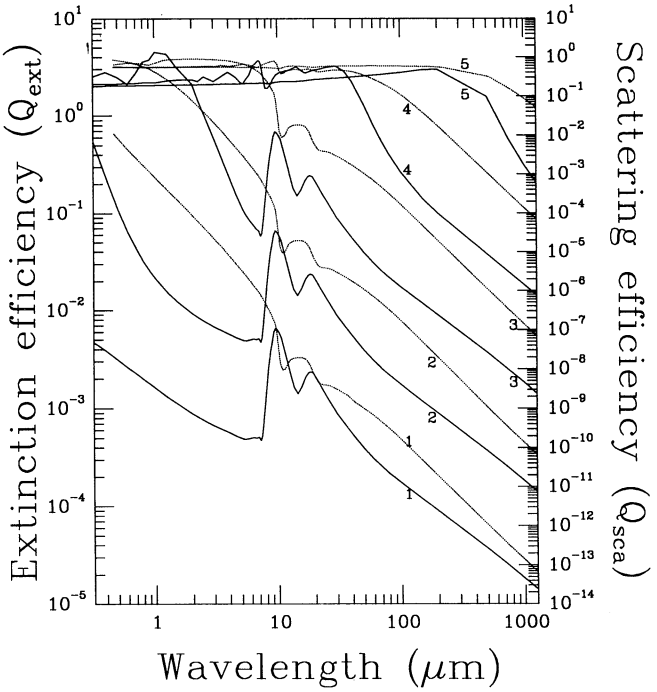

Figure 2. Extinction efficiency, Q_{ext} (solid line) and scattering efficiency, Q_{scat} (dotted line) for grains of various sizes. Curves labelled 1, grain radius = 0.005 μm; 2, radius = 0.05 μm; 3, radius = 0.5 μm; 4, radius = 5.0 μm; 5, radius = 50 μm.

silicate features are more and more flattened out, until by 10-μm radius the extinction and scattering are almost independent of wavelength up to some critical value, longwards of which the absorption efficiency falls roughly as λ^{-1}. Grains with radii in the range 1–10 μm display some interesting structure, but not the usual 10- and 20-μm features, which have saturated and disappeared; structure appears around the points of inflection in the refractive indices. The effects are negligible on model fluxes.

SAO 179815 is classified as K5V (Upgren *et al.* 1972). However it was also noted to be a double star by Heintz (1980), the components being separated by 0.59 arcsec and having a magnitude difference of 0.3 mag. The Upgren *et al.* spectral type may therefore be a composite one. However, in the modelling that follows, we treat the system as a single star. The photovisual V magnitude is taken from Upgren *et al.* (1972), who determined the V magnitude photographically, the *JHKL* photometry is taken from García-Lario *et al.* (1990). All photometry presumably included both stars of the binary system. No secondary spectral type is available, and so since the secondary is fainter we assume it to be an M dwarf and therefore fainter at all wavelengths. The spectral type was used to determine an appropriate temperature and radius for the star, from which a distance was determined by fitting the stellar blackbody continuum to the photometry. We take the radius to be 4.9×10^{10} cm, and the temperature to be 4350 K (Schmidt-Kaler 1982), from which the distance is determined to be 16 pc. The star has no Gliese number.

We constructed a grid of models, varying α and β. In each case the inner radius of the disc was chosen so that the temperature distribution of the grains gave the best fit to the *IRAS* 12- and 25-μm PSC fluxes. The effects of varying α and β are easy to predict. As β is increased, the proportion of the mass of dust in the inner, warmer, part of the disc grows, and so for an acceptable fit to the 12- and 25-μm points the model falls progressively further below the 60- and 100-μm points. Decreasing the value of α increases the proportion of large grains, whose emissivities are roughly constant out to long wavelengths, and thus increases the fluxes at 60 and 100 μm relative to those at 12 and 25 μm. Also, the contrast of the silicate feature at 9.7 μm is decreased, providing us with a further constraint by comparison with our CGS3 spectrum.

In producing the grid of models, we took as standard minimim and maximum grain radii of 0.005 and 100 μm respectively. We varied α between 3.5 and 1.5, and β between 1.0 and 4.0. Resulting best-fitting model values for the dust disc mass and disc inner radius are given in Table 1, along with the corresponding *IRAS* 12-, 25-, 60- and 100-μm fluxes and colour correction factors, and some representative spectra are plotted in Fig. 3. In calculating the *IRAS* fluxes, we have used the published *IRAS* system response curves convolved with a ν^{-1} power spectrum, as was used in generating the *IRAS* Point Source Catalog. Contrast in the silicate feature restricts us to models with α

Table 1. Model results.

Model	α	β	M_{disk} [$M_\odot$]	R_{in} [cm]	F12 [Jy]	corr	F25 [Jy]	corr	F60 [Jy]	corr	F100 [Jy]	corr	r_g(min) [μm]	r_g(max) [μm]
IRAS PSC					2.0±0.2		9.3±0.7		7.2±0.8		4.3±0.5			
M1A	3.5	1.0	2.7×10^{-9}	2.5×10^{13}	2.00	0.85	9.34	1.10	3.42	1.23	1.40	1.10	0.005	100
M1B	2.5	1.0	1.6×10^{-8}	2.8×10^{13}	2.00	0.84	9.38	1.06	7.26	1.10	3.73	1.08	0.005	100
M1C	2.0	1.0	2.7×10^{-8}	1.8×10^{13}	1.99	0.90	9.39	0.99	9.20	1.10	4.73	1.09	0.005	100
M2A	3.5	2.0	3.2×10^{-10}	3.0×10^{13}	2.02	0.85	9.39	1.11	2.78	1.29	0.85	1.16	0.005	100
M2B	2.5	2.0	1.6×10^{-9}	3.2×10^{13}	1.98	0.84	9.25	1.05	6.02	1.15	2.39	1.13	0.005	100
M2C	2.0	2.0	2.6×10^{-9}	2.1×10^{13}	2.01	0.90	9.28	1.00	7.81	1.12	3.51	1.11	0.005	100
M2D	1.5	2.0	2.8×10^{-9}	1.6×10^{13}	2.01	0.91	9.31	0.99	7.83	1.12	3.86	1.09	0.005	100
M3A	2.5	3.0	7.2×10^{-10}	3.4×10^{13}	1.99	0.84	9.28	1.06	5.79	1.15	2.26	1.13	0.005	100
M3B	2.0	3.0	1.0×10^{-9}	2.2×10^{13}	2.01	0.90	9.39	1.00	7.56	1.13	3.26	1.11	0.005	100
M3C	1.5	3.0	1.2×10^{-9}	1.8×10^{13}	1.99	0.91	9.31	0.99	7.44	1.13	3.52	1.09	0.005	100
M4A	2.5	4.0	5.7×10^{-10}	3.6×10^{13}	2.02	0.84	9.24	1.06	5.54	1.16	2.11	1.14	0.005	100
M4B	2.0	4.0	9.4×10^{-10}	2.4×10^{13}	1.99	0.89	9.32	1.00	7.49	1.13	3.21	1.12	0.005	100
M4C	1.5	4.0	1.0×10^{-9}	1.8×10^{13}	2.01	0.91	9.35	0.99	7.24	1.13	3.37	1.10	0.005	100
M5A	2.0	3.0	1.0×10^{-8}	2.2×10^{13}	2.02	0.89	9.27	1.00	7.49	1.13	3.34	1.11	0.005	1000
M5B	2.0	3.0	7.1×10^{-9}	2.1×10^{13}	2.02	0.90	9.28	1.00	7.36	1.13	3.31	1.10	0.5	1000
M5C	2.0	3.0	7.7×10^{-9}	2.2×10^{13}	1.98	0.90	9.36	0.99	7.64	1.13	3.48	1.10	0.05	1000
M5D	2.0	3.0	1.0×10^{-7}	2.2×10^{13}	2.00	0.90	9.30	1.00	7.72	1.13	3.58	1.10	0.005	10000
M5E	2.0	3.0	3.5×10^{-10}	2.8×10^{13}	2.01	0.86	9.22	1.02	8.34	1.10	2.99	1.17	0.005	10

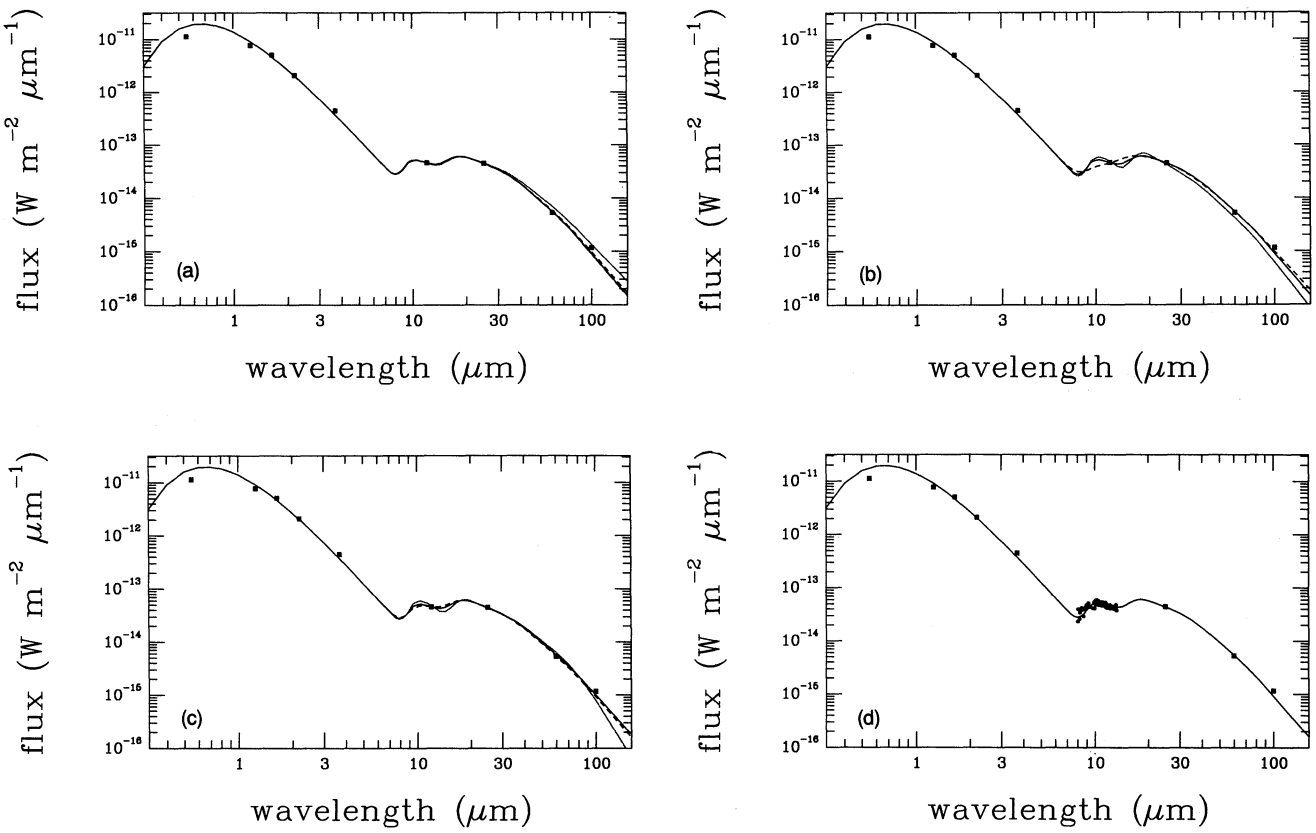

Figure 3. Representative model spectra. Filled squares are photometry as described in the text. (a) The effect of varying β: dotted line is model M1C, dashed line M2C, solid line M3B, dash-dotted line M4B. (b) The effect of varying α: dotted line is M3A, solid line M3B and dashed line M3C. (c) The effect of varying minimum and maximum grain sizes: dashed line is M5B, solid line M5D and dotted line M5E. (d) The best-fitting model, M5A, together with the CGS3 spectrum; *IRAS* fluxes have been colour corrected, and the CGS3 spectrum rescaled to the *IRAS* 12-μm flux.

close to 2.0. Of course, M3B and M4B both have acceptable 60-μm fluxes, but a slight deficiency at 100 μm. M3B offers a slightly better flux distribution, and we regard it as the best model fit. The disc is allowed to extend outward to a point where the dust grain temperatures are less than 30 K, and further extension was found to make no difference to the 100-μm flux.

Finally, having ascertained that values of $\alpha = 2.0$, $\beta = 3.0$ appear to give the best fits to the *IRAS* and CGS3 data, we ran a few further models in which we tried varying the minimum and maximum grain sizes. Increasing the minimum grain size to 0.5 μm had the expected effect of decreasing the contrast of the silicate feature, whilst decreasing the maximum grain size to only 10 μm creates a small increase in the silicate feature contrast, but significantly reduces the far-IR flux. Increasing the maximum grain size to 1 cm produces a comparatively small increase in the far-IR flux at 100 μm, whilst having little effect on the silicate feature at 9.7 μm. In Fig. 3(d) we present model M5A, with the *IRAS* fluxes corrected using the colour corrections calculated for this model, and the CGS3 spectrum rescaled to the corrected *IRAS* 12-μm flux. The inner and outer radii for the model disc in this case are 1.5 and 205 AU respectively. Dust grain temperatures at the inner edge of the disc lie in the range 155–210 K.

4 DISCUSSION

How uniquely can we define the parameters of this disc?

At wavelengths much longer than the radius of an emitting grain, the efficiency of the grain becomes low. We can see this in Fig. 2, where the extinction efficiency falls roughly as λ^{-1} longwards of a critical wavelength equal to $2\pi r_g$. This creates, in the emitted spectrum from a disc having a distribution of grain sizes and temperatures, a shoulder somewhere in the far-IR, beyond which the flux falls off more steeply. The *IRAS* data dictate that this shoulder must occur longwards of or close to 100 μm, and this puts a great constraint on our models. First, the maximum grain size must be at least 10 μm to provide grains with constant absorption efficiency to sufficiently long wavelengths. Secondly, there must be a significant population of these large grains in order to provide sufficient emission at long wavelengths. With a power-law distribution of grain sizes we find it is necessary to extend the size distribution up to at least 100 μm to provide an acceptable fit to the flux at the wavelength of 100 μm. An alternative might be to suppose that there were two distinct populations of small and large grains, such as a distribution of small 'zodiacal' grains, and a massive cloud of comets orbiting far from the star (*cf.* Marochnik, Mukhin & Sagdeev 1988). However, it is unlikely that such a system

would produce such a smooth, monomodal distribution of fluxes from 12 to 100 μm.

Varying the radial dust density distribution also affects the ratio of 25- to 100-μm fluxes. However, if there are insufficient large grains, in order to fit the 100-μm flux by varying the value of β, too much flux is generated at 60 μm due to the shoulder referred to earlier (e.g. model M5E, Fig. 3c).

The contrast of the silicate feature at 9.7 μm disappears very rapidly if the value of α is reduced below 2.0. If the value of α is allowed to rise above 2.5 the contrast increases quite rapidly. Our observations and model constrain the value of α to lie close to 2.0. This tight constraint in turn forces β to lie in the range 3.0–4.0. $\beta = 3.0$ gives the better results, and has the incidental advantage of agreeing with the results of Artymowicz *et al.* (1989) and Becklin & Zuckerman (1990) for various other stars. Thus, of the models M1–M4 in Table 1, M3B gives the best results, and M4B is the only other model in our grid which gives an acceptable model fit.

From the observed contrast of the silicate feature we rule out models where $r_g(\min) > 0.01$ μm, and the best results are obtained by leaving $r_g(\min) = 0.005$ μm (model M5A in Table 1), in accord with the interstellar value (Mathis *et al.* 1977). The maximum grain radius, $r_g(\max)$, is more difficult to constrain. We know, as already mentioned, that it should be at least 100 μm, but to establish some maximum value beyond this we would need observations at longer wavelengths. In the case of SAO 179815 such observations may be possible with large submillimetre telescopes such as the James Clerk Maxwell Telescope (JCMT). From our model M5A we derive fluxes of 220 mJy at a wavelength of 450 μm and 30 mJy at 1-mm wavelength.

For small grains, whilst the cross-sectional area is proportional to r_g^2 and the mass is proportional to r_g^3, the absorption efficiency Q_{abs} is roughly proportional to r_g at wavelengths of interest in the infrared and submillimetre. Therefore the opacity per unit mass of the grains remains roughly constant for all grain sizes. However, for large grains Q_{abs} is independent of grain size for wavelengths less than $2\pi r_g$. The emission in the mid-IR, far-IR and submillimetre in our models is dominated by these large grains, for which the opacity per unit mass is inversely proportional to r_g, and thus as the maximum grain size is increased, so the disc mass must be increased to retain sufficient flux in the IR. This explains the difference in disc masses between models M5A and M5D. Becklin & Zuckerman (1990) quote disc masses for a number of Vega excess type stars. For Vega, they quote a disc mass of 4×10^{-9} $M_\odot$. Given the stellar mass ratio of Vega to SAO 179815, our model M5D derived disc mass of 1.0×10^{-7} $M_\odot$ for SAO 179815 seems unlikely, if such a direct and trivial comparison is reasonable. Before using this as a constraint on grain sizes, we should check that disc masses quoted by Becklin & Zuckerman (1990), who take no account of the effects of variable grain size on their derived disc properties, are consistent with the disc mass obtained by our modelling technique.

Fig. 4 shows the spectrum emitted by the disc alone (i.e. with the stellar photospheric curve removed), compared to a 150-K blackbody. Becklin & Zuckerman use the formula

$$M_d = \frac{KF_\nu D^2}{B(\nu, T)} (\lambda/0.025)^\gamma \qquad (1)$$

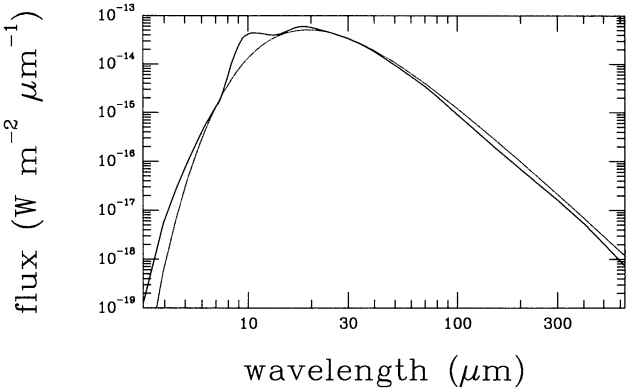

Figure 4. Spectrum emitted by the dust disc alone, with the stellar photospheric contribution removed (solid line), compared to a 150-K blackbody (dotted line).

due to Hildebrand (1983), where λ is in cm and the grain emissivity is proportional to $\lambda^{-\gamma}$ (so that $\gamma = 1$ for our case). Following Becklin & Zuckerman, we take K, the inverse opacity of the dust grains, to be 0.05 g cm^{-2} at a wavelength of 250 μm. $B(\nu, T)$ is the blackbody intensity at 450 μm for a temperature $T = 150$ K. D is the stellar distance, 16 pc, and $F_\nu = 220$ mJy is the model flux at 450 μm, taken from model M5A (for this comparison, and those discussed below, the model disc was allowed to extend outward to where the dust grain temperatures were less than 10 K). Inserting these values, we obtain a disc mass from the Hildebrand formula of 1.2×10^{-8} $M_\odot$.

It is important to note the condition which must be fulfilled in order that the Hildebrand formula may be used – $\lambda \gg 2\pi r_g$. For model M5A, the largest grains have radius 1000 μm. We must therefore determine the model flux at a wavelength much greater than 6.3 mm! At 6.3 mm, the absorption efficiency of the largest grains turns over and begins to fall rapidly; eventually, at some wavelength of the order of 3 times 6.3 mm, the absorption efficiency curve for these largest grains joins the manifold of curves proportional to λ^{-1}, and then for all grains in our model the condition $Q_{abs}/r_g = $ constant is met, and the Hildebrand formula becomes applicable. If in the above calculation for model M5A we replace the value of K with that determined from our own dust data at 450 μm, we derive a disc mass of 5.0×10^{-9} $M_\odot$, a factor of 2 different from that used in our model. The discrepancy arises because Q_{abs}/r_g is not constant at wavelengths as short as 450 μm, rendering Hildebrand's formula inaccurate. This can be tested using our model M5E data. Since the largest grains are only 10 μm in radius, the Hildebrand formula can be applied at wavelengths longer than about 200 μm. We take the flux from model M5E at 1250 μm, and determine K at 1250 μm from our dust data, and from this determine a disc mass from the Hildebrand formula of 3.5×10^{-10} $M_\odot$, which is identical to the mass determined directly from our model. Becklin & Zuckerman, in using their measured fluxes at 450 μm, will have determined accurate disc masses only if the grains in the discs they observed are mainly smaller than about 25 μm. It is thus crucial to determine the range of grain sizes present in the discs around as many Vega-excess stars as possible. It is

impractical with our current data to determine a maximum grain radius; we see that as this value is increased, so the 100-μm flux increases towards that observed. Extrapolating our results in Table 1, we would obtain a disc mass equal to one Jupiter mass with maximum grain radii of about 100 m, or roughly asteroid-sized. At this size the population may well be curtailed, only a small number of larger bodies (planets) being expected, these making a tiny contribution to the total IR flux from the system. These results are quite consistent with, but do not necessarily imply, the existence of a planetary system similar to our own. An important extension of this work in the future should be to apply it to other, similar systems, especially those for which Becklin & Zuckerman obtained 800-μm fluxes. It would be interesting to determine whether disc masses are roughly constant fractions of the parent stellar masses, or whether other factors are involved.

An important potential source of problems is the beamsize. *IRAS* photometry was obtained with very large (several arcmin) beams, whilst our CGS3 spectrum employed a 5.5-arcsec beam. We have investigated the effects of this in our models, and conclude that the disc was completely unresolved by CGS3. A significant decrease in the flux at 12 μm should not occur until the beamsize is reduced below 1 arcsec. Even at 100 μm, where the disc should be at its largest and easiest to resolve, the disc should have been completely unresolved by *IRAS*. This is in accord with the work by Walker & Wolstencroft (1988), who estimated SAO 179815 to have one of the two smallest discs among their sample of stars.

5 CONCLUSIONS

The observation of a broad 9.7-μm silicate feature in the K5V star SAO 179815 has been used to demonstrate that small silicate grains must be present around the star. The system has been modelled as a circumstellar disc, and it has been found that a grain size distribution with minimum radius <0.01 μm and maximum radius at least 100 μm must be present. The grain size distribution is characterized as $n_g \propto r_g^{-2}$, and the dust mass denstiy distribution in the disc is most plausibly modelled as $\rho_g \propto r^{-3}$. The maximum grain size cannot realistically be determined with the available data, but the data are consistent with the existence of a planetary system similar to our own.

ACKNOWLEDGMENTS

CJS acknowledges the financial support of the UK Science and Engineering Research Council in the form of a post-doctoral fellowship. We are indebted to numerous UKIRT staff for their support during and before our observations with CGS3, especially Tom Geballe and Gillian Wright, and also to the editor and an anonymous referee for helpful suggestions. This research used data from the SIMBAD data base, operated at CDS, Strasbourg, France.

REFERENCES

Artymowicz, P., Burrows, C. & Paresce, F., 1989. *Astrophys. J.*, **337,** 494.
Aumann, H. H., 1985. *Publs astr. Soc. Pacif.*, **97,** 885.
Aumann, H. H., Gillett, F. C., Beichman, C. A., de Jong, T., Houck, J. R., Low, F. J., Neugebauer, G., Walker, R. G. & Wesselius, P. R., 1984. *Astrophys. J. Lett.*, **278,** L23.
Becklin, E. E. & Zuckerman, B., 1990. In: *Submillimetre Astronomy,* p. 147, eds Watt, G. D. & Webster, A. S., Kluwer, Dordrecht.
Biermann, P. & Harwit, M., 1980. *Astrophys. J. Lett.*, **241,** L105.
Dohnanyi, J. S., 1969. *J. geophys. Res.*, **74,** 2531.
Dohnanyi, J. S., 1970. *J. geophys. Res.*, **75,** 3468.
Draine, B. T. & Lee, H.-M., 1984. *Astrophys. J.*, **285,** 89.
García-Lario, P., Manchado, A., Pottasch, S. R., Suso, J. & Olling, R., 1990. *Astr. Astrophys. Suppl.*, **82,** 497.
Gillett, F. C., 1986. In: *Light on Dark Matter,* p. 61, ed. Israel, F. P., Reidel, Dordrecht.
Heintz, W. D., 1980. *Astrophys. J. Suppl.*, **44,** 111.
Hildebrand, R. H., 1983. *Q. J. R. astr. Soc.*, **24,** 267.
Marochnik, L. S., Mukhin, L. M. & Sagdeev, R. Z., 1988. *Science,* **242,** 547.
Mathis, J. S., Rumpl, W. & Nordsieck, K. H., 1977. *Astrophys. J.*, **217,** 425.
Paresce, F. & Burrows, C., 1987. *Astrophys. J. Lett.*, **319,** L23.
Schmidt-Kaler, Th., 1982. In: *Landolt–Börnstein, Numerical Data and Functional Relationships in Science and Technology, Group VI, Astronomy, Astrophysics and Space Research,* Vol. 2b, eds Schaifers, K. & Voigt, H. H., Springer-Verlag, Berlin.
Skinner, C. J. & Whitmore, B., 1987. *Mon. Not. R. astr. Soc.*, **224,** 335.
Smith, B. A. & Terrile, R. J., 1984. *Science,* **226,** 1421.
Telesco, C. M. & Knacke, R. F., 1991. *Astrophys. J. Lett.*, **372,** L29.
Telesco, C. M., Becklin, E. E., Wolstencroft, R. D. & Decher, R., 1988. *Nature,* **335,** 51.
Upgren, A. R., Grossenbacher, R., Penhallow, W. S., MacConnell, D. J. & Frye, R. L., 1972. *Astr. J.*, **77,** 486.
Walker, H. J. & Wolstencroft, R. D., 1988. *Publs astr. Soc. Pacif.*, **100,** 1509.